Nucleation and growth of mixed vanadium-titanium oxo-alkoxy nanoparticles in sol-gel synthesis

Miguel Sanchez Mendez, Zixian Jia, Mamadou Traore, Mounir Ben Amar, Mehrdad Nikravech, Andrei Kanaev

Nucleation and growth of mixed vanadium-titanium oxo-alkoxy nanoparticles in sol-gel synthesis

Miguel Sanchez Mendez, Zixian Jia, Mamadou Traore, Mounir Ben Amar, Mehrdad Nikravech and Andrei Kanaev [*]

Laboratoire des Sciences des Procédés et des Matériaux, C.N.R.S., Université Sorbonne Paris Nord, 93430 Villetaneuse, France

[*] Correspondent author. E-mail: andrei.kanaev@lspm.cnrs.fr

Abstract

The mixed vanadium-titanium oxo-alkoxy (VTOA) nanoparticles were synthesized *via* sol-gel method in a chemical reactor with ultra-rapid micromixing. The nucleation and growth kinetics and particles size, followed by the static/dynamic light scattering methods, were quite different from those of pure oxo-alkoxy titanium (TOA) and vanadium (VOA) species. It was shown that the TOA species appear first and serve to be centres of attraction for hydrolysed VOA species at the nucleation stage. However, at the vanadium content above 20 mol% large VOA species imprison sub-nucleus TOA species prohibiting the nucleus appearance. The model analysis of the VTOA induction kinetics validated a significant increase of the nucleus size with an increase of the precursor concentration. The results support a new paradigm of the sol-gel process describing profound restructuring of the oxometallic species during assembling at the nucleation stage.

Keywords: *sol-gel process, vanadium-titanium oxo-alkoxy nanoparticles, static/dynamic light scattering, nucleation-growth kinetics, particle size.*

1. Introduction

The nucleation stage is of paramount importance for the understanding and control of the sol-gel process. Indeed, the nucleus serves to be the smallest stable unit posessing the electronic structure of the macroscopic bulk solid counterpart. In the same time, its large surface-to-volume ratio leads to many consequences of the fundamental caracter connected to energetic, quantum, electronic, electrodynamic, thermodynamic, etc. size effects, which describe the gradual "transition" from the molecular to infinite bulk system [1]. The particularities of the this transition create unique opportunities for tailoring and controlling functional response of the material, e.g. in the fields of catalysis and photocatalysis. Moreover, the material doping at the nucleation stage may offer the possibility of stabilisation of new phases with compositions inaccessible in bulk solids in the ambient (P,T) conditions.

Despite of a long history of the related research [2, 3], the nucleation-growth stage of the sol-gel process has not received a necessary attention. This can be partially explained by a limited power of calculation methods, which are restricted to small clusters of radius below 1 nm [4-6] and synthesis with a significant polydispersity of the condensed species, making unrealistic monitoring of a selective size population evolution. Moreover, the most effective light scattering methods of the insitu nanoparticles observation provide a weak signal in the Rayleigh size domain ($R<<\lambda$) due to the scattered light intensity $I \propto m^2$, where m is the particle mass. In practice, the related studies concern rather large particles ~100 nm [7], which are significantly bigger than those required for the nucleation process analysis.

The LaMer's model [8] initially used for the description of the induction kinetics of the sol-gel process has been rejected in later studies [9], showing the hierarchical growth of the

condensed oxo-alkoxy species. Later on, based on the experimental approach permitting point-like reaction conditions in presence of the ultra-rapid micromixing of the reactive fluids, Rivallin et al. [10] have proposed a description of the induction kinetics of the titanium oxo-alkoxy (TOA) species. This model considers simultaneous hydrolysis and condensation reactions between the nuclei [11]. The more detailed analysis of the reaction kinetics has been not possible up to now, because of the lack of experimental data about the hydrolysis and condensation reaction constants. This model has been later refined [12] and extended to zirconium oxo-alkoxy (ZOA) system [13]. The TOA nucleus size 2R=2.5 nm proposed in early studies has been later revised: 2R=3.2 nm [14], which has been independently supported by HRTEM analysis of the titania-based organic-inorganic hybrid materials [15].

Despite of a seeming simplicity, the hydrolysis and condensation reactions, successively involving different alkoxy and hydroxy groups of a metal cation, are complex and progress simultaneously prohibiting their separate analyses. In confirmation, the related studies were limited to an estimation of the overall process time, as e.g. reported in the well-known paper by Livage et al. [16]. This classical picture of the kinetically controlled hydrolysis-polycondensation process has been recently reconsidered as not realistic. In contrast, the new paradigm states that the process results directly in well-defined oligonuclear oxo-alkoxide species through one-step hydrolysis-condensation transformation associated with profound restructuring of the oxometallate species as the reactions progress [17, 18]. However, such continuous transformation inherent to the molecular species may not be extended to nanoparticles and the limit size particle can exist, which cohesive energy prohibits the system reforming. The notion of a stable nucleus becomes in this connection of a particular importance, since it designates the ultimate species capable to withstand the

restructuring and link to the bulk crystalline solids properties. In support of this statement, correlations between the nucleus composition, size, phase transformation temperature and crystalline phase have been demonstrated in bicationic zirconium-titanium oxo-alkoxy (ZTOA) species [19]. It is also intriguing that the nucleus size of TOA species corresponds to the smallest size of TiO_2 crystallites R=1.5 nm, which electronic band structure converges to that of the bulk TiO_2 solid [20-21]. The role of pre-nucleation clusters as solute precursors in the emergence of new phases has been highlighted in a review paper [22]. Summing up, further studies of the nucleation-growth kinetics are required in order to better understand still non-elucidated mechanisms of the solid formation in sol-gel process.

In this communication we report on the kinetic studies of the nucleation and growth process of vanadium-titanium oxo-alkoxy (VTOA) species. In contrast to the previously considered ZTOA species, which have distinct counterpart solid solutions $Zr_xTi_{1-x}O_2$ ($0.0 \leq x \leq 1.0$), $V_xTi_{1-x}O_2$ solid solutions in the range of $0 \leq x \leq 1$ compositions remain an issue. In fact, the phase equilibrium of the Ti-V-O system has been extensively studied in the past, showing no reliable support of their existence in the ambient (P,T) conditions [23]. The interest to these mixed oxide solids is significant in connection with the band gap engineering and potential applications in catalysis, photocatalysis, energy storage, etc. [24-29]. An extension of the previously discussed nucleation and growth mechanism to the VTOA system completes this experimental work.

2. Experiment and sample preparation

The experiments were realized in an original laboratory-scale sol-gel reactor with ultrarapid micromixing of the reaction medium [10, 30]. In brief, two injection volumes of the reactor

contained stock solutions with (1) precursors and (2) water in the same alcohol solvent (n-propanol in this work) were maintained at the temperature of 20.0 °C using a thermo-cryostat Haake DC10K15. These solutions, each of 50 ml volume, were prepared in a LABstar glove box workstation MBraun (traces of oxygen and humidity ≤0.5 ppm) and transferred to the injection volumes of the reactor via glass syringes maintained under dry nitrogen gas flow, in order to avoid any contamination by air humidity and dust particles capable affecting the process kinetics. The titanium tetraisopropoxide (TTIP, 98% purity, Sigma-Aldrich) and vanadium(V) oxytripropoxide (VOP, 98% purity, Sigma Aldrich) precursors, n-propanol solvent (99.5% purity, Sigma-Aldrich), and distilled twice-filtered water (syringe filter 0.2 lm porosity PALLs Acrodisc) were used in the preparation procedure. The total precursor concentration $C_0=C_{Ti}+C_V$ in the reaction medium, with the vanadium fraction $d(\%)=C_V/C_0/100$, was adjusted to 0.15 mol/l or 0.3 mol/l in most of the experiments and concentration of water C_w corresponded to the hydrolysis ratio $H=C_w/C_0$ varied between 1.5 and 5. The reactions began after the synchronous injection (with ~5 ms precision) of the stock solutions in a T-mixer via two exocentric input arms of 1 mm internal diameter and an output tube of 2 mm internal diameter. The injected fluid with Reynolds number Re=6000 ($Re=4Qp/\pi\eta d$, where Q, p and η are flow rate, density and dynamic viscosity of the fluid respectively) formed the zone of a strong turbulence forcing the solutions to mix at the molecular level on a timescale $t_{mix}<10$ ms, which is shorter than the characteristic time of chemical reactions resulting in the particles nucleation t_{nuc}. This reactor regime corresponds to so-called small Damköhler numbers $Da= t_{mix}/t_{nuc}\leq 1$, which assure point-like conditions in the reaction medium with perfectly homogeneous composition, which permits the narrowest polydispersity of the produced nanoparticles. The experiments were carried out under a continuous dry nitrogen gas flow and fixed temperature of 20 °C.

The hydrodynamic particle's size (2R, nm) and scattered light intensity (I, Hz) in the reaction medium were continuously monitored respectively by DLS (dynamic light scattering) and SLS (static light scattering) methods, using 40 mW / 640 nm single-frequency laser Cube 640-40 Circular (Coherent). The laser light was transferred to the colloid and to the analyzing equipment via a home-made monomode optical fiber probe, assuring a small observation volume of ~10^{-6} cm^3 in order to avoid multiple scattering events even in high-concentration colloids. The received signal was treated with a 48 bits / 288 channels photon correlator Photocor-PC2 (PhotoCor Instruments). In each experimental series, the measurements were carried out in the automatic sampling mode each minute during 2-4 hours; the accumulation period of 60 s permitted rejection of non-desirable strong scattering spikes due to rare dust particles and resolving a weak signal from nanoparticles with a good signal-to-noise ratio. The reliable range of the particle size measurements $R \geq 1.0$ nm was defined by the internal auto-correlation response of the PhotoCor photomultiplier. The particle radius R was calculated from the least-squared fit of the experimental ACF data by one- (i=1) and two- (i=2) exponential decay functions $y=y_0+\Sigma a_i e^{-t/\tau i}$ (i=1, 2) using the Stokes-Einstein relation $R(nm)=7.14 \cdot 10^4 \tau$ (s) in our experimental conditions.

3. Results and Discussion

The pure TOA and VOA systems show strongly different reaction kinetics and particles polydispersity. While TOA nanoparticles appear almost instantaneous after the reactive fluids injection forming nucleus of size $2R_{TOA}=3.2$ nm, the population of VOA species of a large size ≥200 nm steadily grows after the injection. At the same time, preliminary experiments have indicated a strong interaction between TOA and VOA systems when the respective precursors are introduced in the same n-propanol solution [31].

Our DLS measurements in Fig. 1 showed that the decay time of ACF curves increases with an increase of the vanadium content, which according to the Stokes-Einstein relation signifies an increase of the particles size (2R) and mass (m). At the same time, in contrast to the expected stronger light intensity (I) scattered from larger particles ($I \propto m^2$ in the Rayleigh domain $\lambda >> R$), the signal-to-noise ratio significantly decreased. This clearly indicates a decrease of the nanoparticles concentration, once more surprising since the vanadium addition was relatively small (≤10 mol%) and the hydrolysis ratio was larger than that critical one $h^*=1.5$ needed for the homogeneous TOA nucleation [12]. This can be explained by a competitive water consumption of Ti and V precursors. Indeed, at the complete hydrolysis vanadium(V) precursor with d=2 mol% can consume about all excessive water above that required for the TOA nucleation: $5d/100=0.1=H-h^*$; the hydrolysis of d=10 mol% vanadium(V) precursor consequently decreases the free water concentration in the solution by 5d/100=0.5 mol% down to $H' \approx 1.2 < h^*$ supressing TOA nucleation [12]. This is supported by a progressive decrease of the signal-to-noise ratio of ACF curves in Fig. 1 from a (d=0) to d (d=10 mol%). We notice that the faster hydrolysis kinetics of V species compared to that of Ti species is in agreement with the elements electronegativity on the Pauling scale: respectively 1.63 (V) and 1.54 (Ti). Based on these observations, conclusions can be drawn that (i) vanadium species effectively hydrolysed, strongly consuming free water in the solution and preventing homogeneous TOA nucleation and (ii) mixed oxide VTOA particles nucleate owing to the condensation reactions between hydrolysed titanium and vanadium molecular bonds. Moreover, since only rare large VOA species appeared in the absence of the titanium precursor (iii) at d≤10 mol% TOA particles nucleate first, serving an attractor for hydrolysed vanadium molecular species; the nucleus size therefore increases with the vanadium content in the reactive solution. In contrast, (iv) at high vanadium concentrations

above 20 mol% VOA species percolate by imprisoning sub-nucleus TOA species, which prohibits observation of the small nanoparticles.

Further confirmation of the proposed hypothesis can provide measurements of the induction kinetics of the sol-gel process involving VTOA species. The solutions remained highly transparent during this common stage of the sol-gel process and became abruptly opaque at the end, indicating powder precipitation. The temporal evolution of the scattered light intensity in the solutions with 2 mol% V and different H is shown in Fig. 2. In agreement with the general picture of the sol-gel process, the induction period t_{ind} shortened with an increase of H, which can be ascribed to agglomeration of metal oxo-alkoxy nanoparticles. In situ DLS measurements of the particles size shown in Fig. 3 confirmed the appearance of nanoparticles and their slow growth during the induction period. The induction time t_{ind} can be empirically evaluated as a time when the scattered light intensity from the solution increases 5 times over that in the process beginning after the nucleation: $I(t_{tind})=5I(0)$ [32]. At this moment the bimodal particle size distribution appeared, with the smallest particles being weakly aggregated nuclei and large particles of radius above 200 nm grown by feeding from the small nanoparticles population. We notice that few very large (μm size) dust particles can contaminate the solutions at the early process times, which however do not affect the process kinetics. The attachment of small to large particles makes appearing the smallest nucleus fraction, which is generally screened by the aggregates. This can be seen in Fig. 3 as an effective decrease of the small particles size at $t>t_{ind}$. The correlation between the induction rate defined by $r_{ind} =t_{ind}^{-1}$ and initial slope of the particles growth kinetics dR/dt will be discussed below.

The mechanism of the nanoparticles agglomeration in the sol-gel process proposed by Rivallin et al. [10, 11] consists in *n* condensation between surface hydroxyls of two contacting nanoparticles:

$$(\ldots)\text{–}OH^{i} + OH^{i}\text{–}(\ldots) \leftrightarrow / \rightarrow H_2O + (\ldots)\text{–}O^{i}\text{–}(\ldots) \quad (1)$$

which is partially reversible: the process is at equilibrium ($\leftrightarrow$) at $i<k$ and becomes irreversible ($\rightarrow$) after $i \geq k$ consecutive condensation steps, where k is the critical step. This sufficiently simple assumption has provided a successful explanation of the experimental induction rates empirically approximated by

$$r_{ind} \propto k\, C_{Ti}^{\beta}\, (H - h^{*})^{\alpha} \quad (2)$$

where h^{*} stands for the critical hydrolysis ratio, which permits nucleation. This h^{*} corresponds to the condensation ratio of the smallest particle (nucleus) assembling about thousand atoms, which elementary chemical composition in case of TOA (h^{*}=1.5) can be represented by $TiO_{1.5}OR$. This model has been initially proposed for TOA species ascribing α=2n-k-1 and $\beta=\alpha+1$ with the solution in integer values n=3 and k=2 [12]. Later on, the validity of the model has been confirmed for ZOA [13] and mixed oxide ZTOA [19] species.

The validity of expression (2) was verified for the experimentally observed VTOA induction kinetics. The induction rate (r_{ind}) and nanoparticle growth (dR/dt) rates versus the overcritical hydrolysis ratio H-h^{*} are plotted in the logarithmic frame in Figs 4a and 4b. In both cases, the power law was confirmed with h^{*}=1.5 and power factor $\alpha \approx 5$, which are characteristic of the TOA nanoparticles aggregation and therefore support the assumption of TOA nucleation. However, absolute values of the induction rate were more that an order of magnitude smaller compared to those of TOA nanoparticles in similar experimental conditions. In fact, for H=2.3 (which corresponds to H-h^{*}=0.8 in Fig. 4) TOA induction rate of 0.1 min^{-1} has been observed

[14], while the extrapolation of our experimental data predicts the rate of ~10^{-4} min^{-1}, which according to Eq. 2 results in a much smaller induction rate of ~0.006 min^{-1} in the experimental conditions with 2 times higher Ti precursor concentration (similar to that of VTOA). One can conclude that VTOA induction kinetics is significantly slower than that of TOA.

In confirmation of this conclusion, Fig. 5 shows measured induction times as a function of the vanadium concentration in the solution, which was clearly increased with an increase of C_V. The least squared fit of the experimental data permitted to approximate the induction rates by a power law of C_V and, consequently, rewrite Eq. (2) as:

$$r_{ind} = k\, C_{Ti}^{\beta}\, (H - h^*)^{\alpha}\, C_V^{-\gamma} / (c + C_V^{-\gamma}) \qquad (3)$$

with α=5, β=6 and γ=1.7 obtained from the experiment. While power factors α and β were explained in the model, physical meaning of the empirically introduced parameter γ has to be understood. We also notice that the factor $1/(c+C_V^{-\gamma})$ was introduced in Eq. (3) to avoid singularity at C_V=0.

The particle size underwent a small evolution with the water addition above the critical value h^*=1.5 enabling the nucleation. Two experimental series with 2 mol% and 10 mol% vanadium are shown in Fig. 6. After 2 mol% V addition, the initial radius of the produced particles was about R_0=2.1 nm for H≤3.0 and seemingly increased by 0.4 nm with the following increase of H to 3.6. In contrast, the series with the higher vanadium content of 10 mol% showed significantly increased initial particle radius of R_0=4.3 nm. We notice rather large error bars in this last series, except for the first point accumulated for a long time from an almost stable solution (t_{ind}>6 hours). According to the model [10-11], free water remaining after the nucleation stage promotes the particle aggregation; the influence of water content on size and composition of the elementary nucleus is almost negligible. Apparently, these smallest VTOA particles fit the

nucleus definition, remaining stable with the moderate change of H. More confirmation to an assignment of the hydrodynamic radius 2.1 nm to VTOA nucleus provide experiments performed at a very low hydrolysis ratio close to the critical one, H=1.6 presented in Fig. 7. These series were performed with a higher precursor concentration 0.3 mol/l, in order to increase the nucleus number density, and the very long period of the colloid stability (almost infinite in our experimental conditions) permitted a long ACF data accumulation with a high signal-to-noise ratio. These results indicated that an addition of vanadium above 1 mol% in the sol-gel solution resulted in a stable nucleus of radius R_{nuc}=2.1 nm, which corresponds to that measured in experiments at high $H>>h^*$ in the beginning of the induction period. The induction period can thus be assigned to the aggregation of VTOA nuclei, which confirms the general picture of the sol-gel process described by the Rivallin's model [10].

A further inspection of the model predictions was realised in experiments with an increase of the total precursor concentration, by keeping fixed all other experimental conditions. The experimental SLS data presented in Fig. 8 were realised with the vanadium content of 10 mol%, two hydrolysis ratios of H=4.3 and 4.5 and the total precursor concentration increased from C_0=0.150 to 0.165 mol/l. The small difference in H in this series is explained by the very high sensitivity of the induction time to this parameter. The observed elongation of the induction period with the increase of H perfectly fitted the model prediction by Eq. (3). On the other hand, the induction time was unexpectedly increased with the increase of precursor concentration by 25±5 % in these experiments, which is in a seeming contradiction with the model predicted the induction time shortening at higher precursor concentration. The Rivallin's model is however based on the assumption about fixed nucleus size, which required verification in case of VTOA species. Our complementary DLS measurements showed an increase of radius of the initially

formed VTAO nanoparticles with the increase of C_0 from R_0=5.2±0.7 nm to 7.6±0.7 nm (H=4.3) and from 6.7±0.9 nm to 8.8±1.1 nm (H=4.5). Taking into account the increase of a precursor concentration and nucleus volume, the nucleus concentration is expected to decrease by a factor of ~2.2. In these conditions, Eq. (2) predicts a slowing of the induction rates by ~30%, which corresponds to the experimental observations. The performed experiments suggest that an empirically introduced parameter γ in Eq. (3) is linked to modifications of the nucleus size with an increase of the vanadium concentration. In the same time, the understanding of chemistry background for these modifications requires further studies.

We point out that present results may serve first experimental validation of a new paradigm of the sol-gel process proposed by Kessler [17] in the range of relatively large oxo-alkoxy nanoparticles (R>1 nm). They indicate that VTOA nucleus is adapting to the environment conditions: its size increases with an increase of water (weakly) and precursor (strongly) concentrations. This process, linked to structural modifications, may have consequences on the electronic structure and functional properties of the derivative solids. The work is in progress to provide more information about functional properties of the obtained mixed metal oxide solids.

Based on the obtained results, the picture of the nucleation process is the following. At a small vanadium content ≤10 mol%, TOA nucleates accommodating hydrolysed molecular species of VOA forming nucleus of size, which increases with an increase of the V/Ti ratio. In contrast, at a large vanadium content >20 mol%, hydrolysed vanadium species trap sub-nucleus species of TOA, prohibiting the appearance of small nanoparticles; in these conditions large TOA-including VOA species with a poor defined size are formed. This picture is schematically presented in Fig. 9. Because a net correlation between ZTOA nucleus composition, size and the crystalline phase of $Zr_xTi_{1-x}O_2$ solid solutions has been previously established [19], an absence of

a well-defined nucleus of VTOA for compositions x=V/Ti>0.25 also correlates with non-observed $V_xTi_{1-x}O_2$ solid solutions at the ambient pressure and temperature [23]. Further studies in this field may emerge a valuable prediction method of stable nanocrystalline solids.

4. Conclusion

In conclusion, the mixed vanadium-titanium oxo-alkoxy (VTOA) nanoparticles were synthesized *via* sol-gel method in a rapid micromixing reactor, permitting point-like reaction conditions and narrowest particle size distribution. The particles nucleation and growth kinetics were monitored in situ via home-made monomode optical fibre probe, using static and dynamic light scattering methods. The vanadium addition worsened the coherent component of the scattered light prohibiting the particle size analysis at high vanadium content. However, at relatively low vanadium content ≤10 mol% an analysis of the experimental data permitted to conclude about nucleation of the mixed VTOA particles of 2.1 nm radius. We showed that titanium oxo-alkoxy (TOA) species appear first and serve to be centres of attraction for hydrolysed vanadium oxo-alkoxy (VOA) species at the nucleation stage. In contrast, at high vanadium content VOA species percolate by imprisoning sub-nucleus TOA species prohibiting the nanoparticles appearance. This is connected to stronger hydrolysis and weaker condensation abilities of VOA species compared to TOA. The experimental VTOA kinetics at the induction stage agreed with the Rivallin's model and extended it to the case of non-conservation of the nucleus number density (under fixed total mass of the nuclei). The analysis of the experimental data validated an increase of the VTOA nucleus size with an increase of hydrolysis ratio (weak) and vanadium content (strong); this corresponds to a decrease of the nucleus number density in the reactive solution resulting in the unusual induction time lengthening. The experimental data

support the new paradigm of the sol-gel process proposed by Kessler [17], which assumes a profound restructuring of oxometallic species during their association at the nucleation stage. This restructuring, quite appreciable in heterocationic species M_1M_2OA ($M_1 \neq M_2$=Zr, Ti, V, etc.), can be followed at the particles nucleation stage as a function of the elemental composition.

Acknowledgments

The authors are grateful to Xiaoyan Xie (ENPC) for a software support in treatment of large massifs of experimental data. Miguel Sanchez Mendez acknowledges the financial support of his PhD work by the National Council on Science and Technology (CONACYT) of the Mexican gouvernment and the Doctoral School of the Sorbonne Paris-Nord University.

References

[1] J. Jortner, "Cluster size effects", Z. Phys. D **24**, 247-275 (1992).

[2] C. J. Brinker, G. W. Scherer, *Sol-Gel Science: The Physics and Chemistry of Sol-Gel Processing*, Academic Press, New-York, 1990.

[3] A. C. Pierre, *Introduction to Sol-Gel Processing*, Kluwer Int. Ser. in Sol-Gel Processing: Technology and Applications, Kluwer, 1998.

[4] L. Rozes, N. Steunou, G. Fornasieri, C. Sanchez, "Titanium-oxo clusters, versatile nanobuilding blocks for the design of advanced hybrid materials", Monatshefte für Chemie 137 (2006) 501-528.

[5] Ginger E. Sigmon and Amy E. Hixon, "Extension of the plutonium oxide nanocluster family to include {Pu16} and {Pu22}", Chem. Eur. J. 25 (2019) 1-5.

[6] F. G. Svensson, G. Daniel, C-W. Tai, G. A. Seisenbaeva, V. G. Kessler, "Titanium phosphonate oxo-alkoxide “clusters”: solution stability and facile hydrolytic transformation into nano titania", RSC Adv. 10 (2020) 6873-6883.

[7] A. Forgács, K. Moldován, P. Herman, E. Baranyai, I. Fábián, G. Lente**,** J. Kalmár, "Kinetic model for hydrolytic nucleation and growth of TiO_2 nanoparticles", J. Phys. Chem. C 122 (2018) 19161-19170.

[8] V. K. LaMer and R. H. Dinegar, "Theory, production and mechanism of formation of monodispersed hydrosols", J. Am. Chem. Soc. 72 (1950) 4847-4854.

[9] A. Soloviev, H. Jensen, E.G. Søgaard, A.V. Kanaev, "Aggregation kinetics of sol-gel process based on titanium isopropoxide", J. Mater. Sci. 38 (2003) 3315-3318.

[10] M. Rivallin, M. Benmami, A. Kanaev, A. Gaunand, "Sol-gel reactor with rapid micromixing: modelling and measurements of titanium oxide nano-particles growth", Chem. Eng. Res. Design, 83(A1) (2005) 67-74.

[11] M. Rivallin, M. Benmami, A. Gaunand, A. Kanaev, "Temperature dependence of the titanium oxide sols precipitation kinetics in the sol-gel process", Chem. Phys. Lett. 398 (2004) 157-162.

[12] R. Azouani, A. Soloviev, M. Benmami, K. Chhor, J.-F. Bocquet, A. Kanaev, "Stability and growth of titanium-oxo-alcoxy $Ti_xO_y(O^iPr)_z$ clusters", J. Phys. Chem. C 111 (2007) 16243 - 16248.

[13] S. Labidi, Z. Jia, M. Ben Amar, K. Chhor, A. Kanaev, "Nucleation and growth kinetics of zirconium-oxo-alkoxy nanopparticles", Phys. Chem. Chem. Phys. 17 (2015) 2651-2659.

[14] K. Cheng, K. Chhor, A. Kanaev, "Solvent effect on nucleation-growth of titanium-oxo-alkoxy nanoparticles", Chem. Phys. Lett. 672 (2017) 119-123.

[15] E. Evlyukhin, L. Museur, A. P. Diaz Gomez, M. Traore, O. Brinza, A. Zerr, A. Kanaev, "Synthesis of organic-inorganic hybrids via high-pressure-ramp process: Effect of inorganic nanoparticles loading on structural and photochromic properties", Nanoscale 10 (2018) 22293-22301.

[16] J. Livage, M. Henry, C. Sanchez, "Sol-gel chemistry of transition metal oxides", Prog. Solid State Chem. 18 (1988) 259-341.

[17] V. G. Kessler, "The chemistry behind the sol–gel synthesis of complex oxide, nanoparticles for bio-imaging applications", *J. Sol-Gel Sci. Technol.*, 2009, **51**, 264.

[18] G. A. Seisenbaeva, V. G. Kessler, "Precursor directed synthesis – “molecular” mechanisms in the soft chemistry approaches and their use for template-free synthesis of metal, metal

oxide and metal chalcogenide nanoparticles and nanostructures", *Nanoscale*, 2014, **6**, 6229-6244.

[19] K. Cheng, K. Chhor, O. Brinza, D. Vrel, A. Kanaev, "From nanoparticles to bulk crystalline solid: Nucleation, growth kinetics and crystallisation of mixed oxide $Zr_xTi_{1-x}O_2$ nanoparticles", Cryst. Eng. Comm. 19 (2017) 3955-3965.

[20] S. Monticone, R. Tufeu, A.V. Kanaev, E. Scolan and C. Sanchez. "Quantum size effect in TiO_2 nanoparticles: does it exist?", Appl. Surf. Sci., 162-163 (2000) 565-570.

[21] N. Satoh, T. Nakashima, K. Kamikura, K. Yamamoto, "Quantum size effect in TiO_2 nanoparticles prepared by finely controlled metal assembly on dendrimer templates", Nature Nanotechnology, 3 (2008) 106-111.

[22] D. Gebauer, M. Kellermeier, J. D. Gale, L. Bergström, Helmut Cölfen, "Pre-nucleation clusters as solute precursors in crystallisation", Chem. Soc. Rev. 43 (2014) 2348-2371.

[23] Y. Yang, H. Mao, H-L. Chen, M. Selleby, "An assessment of the Ti-V-O system", J. Alloys Compounds 722 (2017) 365-374.

[24] C. Gannoun, R. Delaigle, A. Ghorbel, E. M. Gaigneaux, "V_2O_5/TiO_2 and V_2O_5/TiO_2-SO_4^{2-} catalysts for the total oxidation of chlorobenzene: one-step sol gel preparation vs two-step impregnation", Cat. Sci. Technol. 9 (2019) 2344-2350.

[25] J. Liu, R. Yang, S. Li, "Preparation and characterization of the TiO_2-V_2O_5 photocatalyst with visible-light activity", Rare Met. 25 (2006) 636-642.

[26] L. Xie, P. Liu, Z. Zheng, S. Weng, J. Huang, "Morphology engineering of V_2O_5/TiO_2 nanocomposites with enhanced visible light-driven photofunctions for arsenic removal", Appl. Cat. B 184 (2016) 347-354.

[27] P. Ngaotrakanwiwat, V. Meeyoo, "TiO_2-V_2O_5 nanocomposites as alternative energy storage substances for photocatalysts, J. Nanosci. Nanotechnol. 12 (2012) 828-833.

[28] R. V. S. S. N. Ravikumar, D. Sundeep, A. G. Krishna, S. D. Ephraim, M. A. Ali, S. I. Ahmed, K. S. Manikanta, T. V. Kumar, "Spectral investigation of structural and optical properties of mechanically synthesized TiO_2-V_2O_5 nanocomposite powders", Materials Today: Proceedings 3 (2016) 31-38.

[29] Y. Wang, J. Zhang, L. Liu, C. Zhu, X. Liu, Q. Su, "Visible light photocatalysis of V_2O_5/TiO_2 nanoheterostructures prepared via electrospinning", Mater. Lett. 75 (2012) 95-98.

[30] R. Azouani, A. Michau, K. Hassouni, K. Chhor, J.-F. Bocquet, J.-L. Vignes, A. Kanaev "Elaboration of pure and doped TiO_2 nanoparticles in sol-gel reactor with turbulent micromixing: application to nanocoatings and photocatalysis", Chem. Eng. Res. Design 88 (2010) 1123-1130.

[31] M. Sanchez Mendez, K. Cheng, M. Traore, M. Ben Amar, A. Kanaev, "Elaboration of mixed oxide photocatalysts", Chem. Eng. Trans. 74 (2019) 433-438.

[32] A. Soloviev, PhD thesis, University Paris 13, Villetaneuse, France, 2000.

Figures

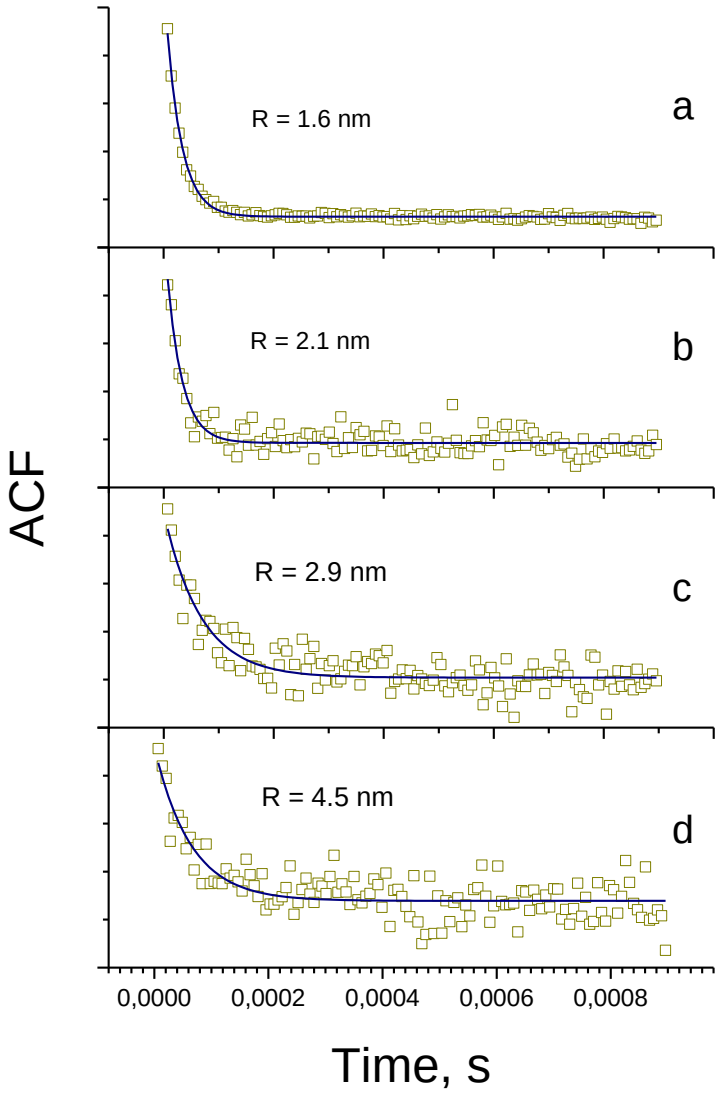

Figure 1: ACF curves of TOA, (a) and VTOA nanoparticles with vanadium content 2 mol% (b), 5 mol% (c) and 10 mol% (d). Preparation conditions: C_0=0.146 mol/l, n-propanol solvent, Re=6000, T=20 °C and H=1.6 (a), 2.5 (b), 3.2 (c), 3.7 (d). Accumulation time 50 x 1 min.

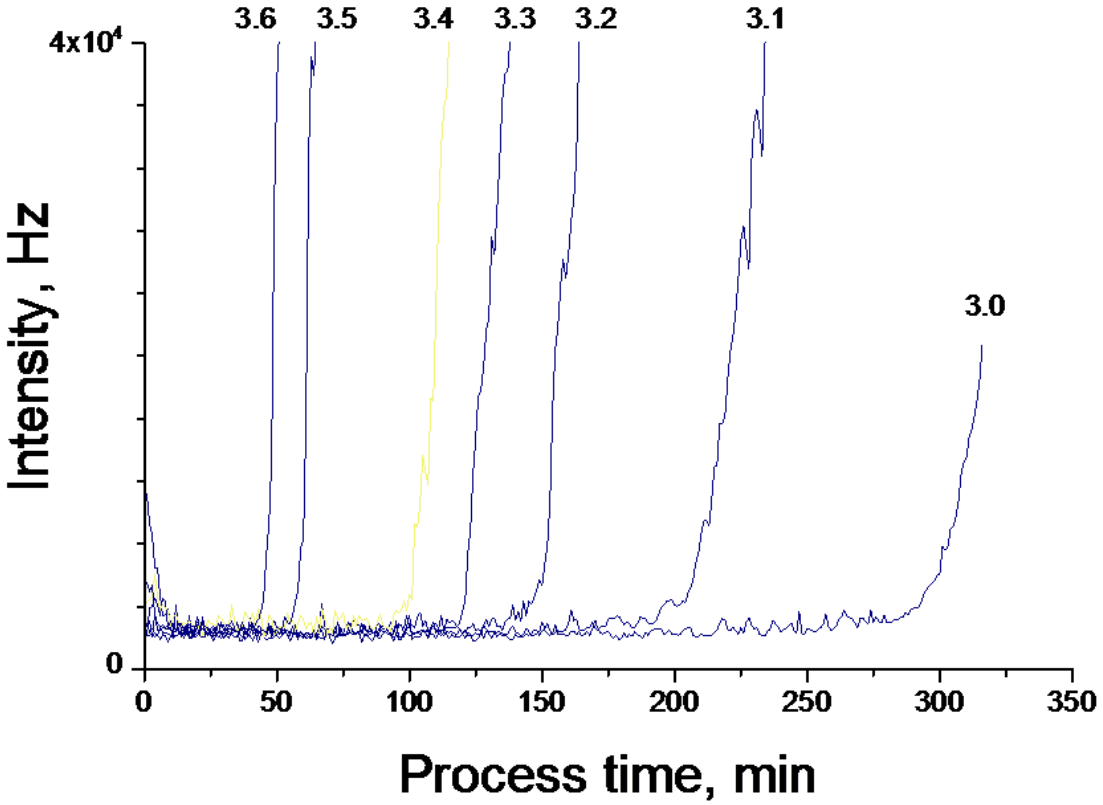

Figure 2: Scattered light intensity during induction period of VTOA nanoparticles growth (C_0=0.15 mol/l, 2 mol% V, n-propanol solvent, Re=6000, 20 °C). Hydrolysis ratios are indicated. Accumulation time 1 min.

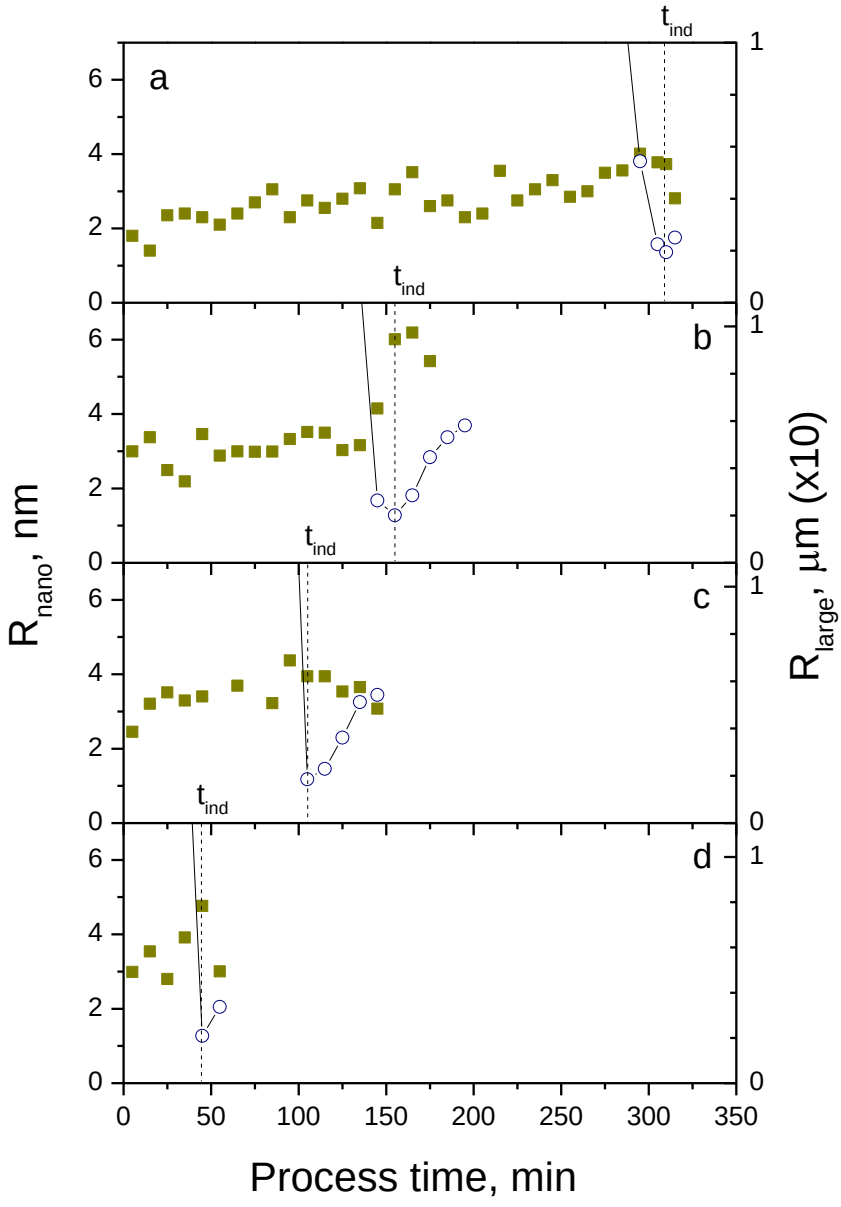

Figure 3: Evolution of radius of VTOA nanoparticles (R_{nano}, ■) and appearance of large agglomerates (R_{large}, ○) on the induction stage of the growth. Preparation conditions: C_0=0.15 mol/l, 2 mol% V, n-propanol solvent, Re=6000, 20 °C, and H=3.0 (a), 3.2 (b), 3.4 (c) and 3.6 (d). Accumulation time 10 x 1 min.

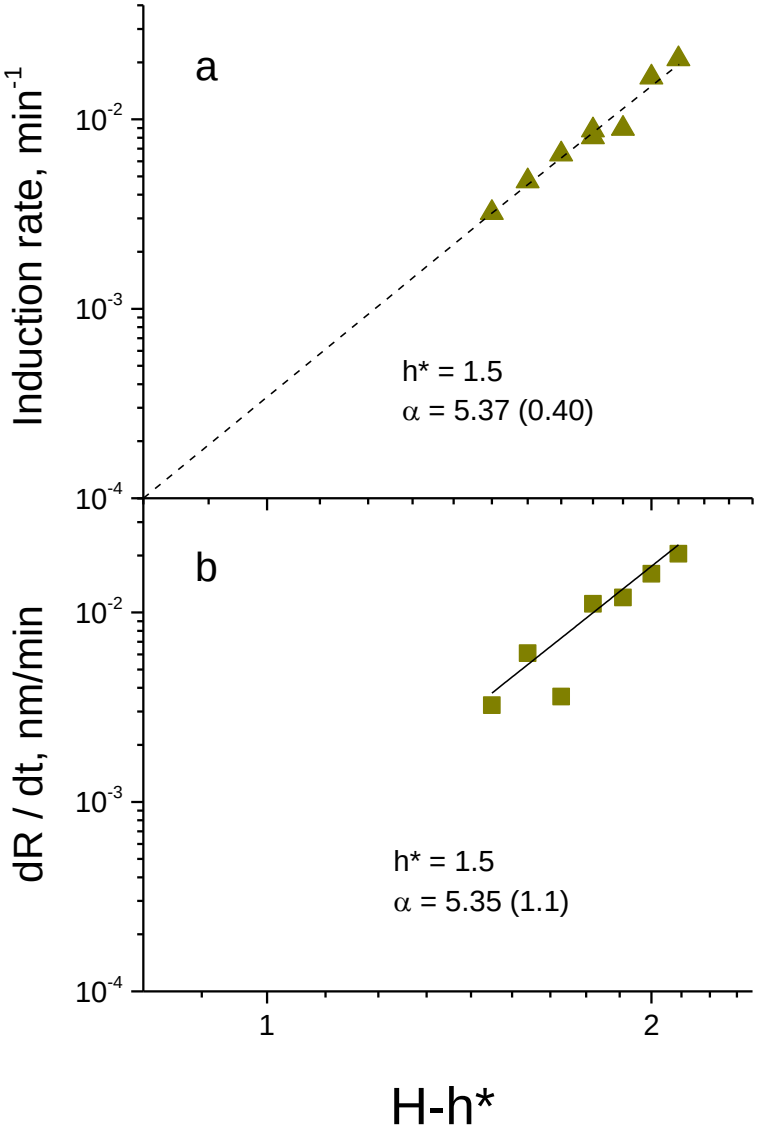

Figure 4: Induction rate (a) and rate of the particle growth (b) versus excessive hydrolysis ratio H-h* over critical one h*=1.5, which leads to TOA nucleation (C_0=0.15 mol/l, 2 mol% V, n-propanol solvent, Re=6000, 20 °C).

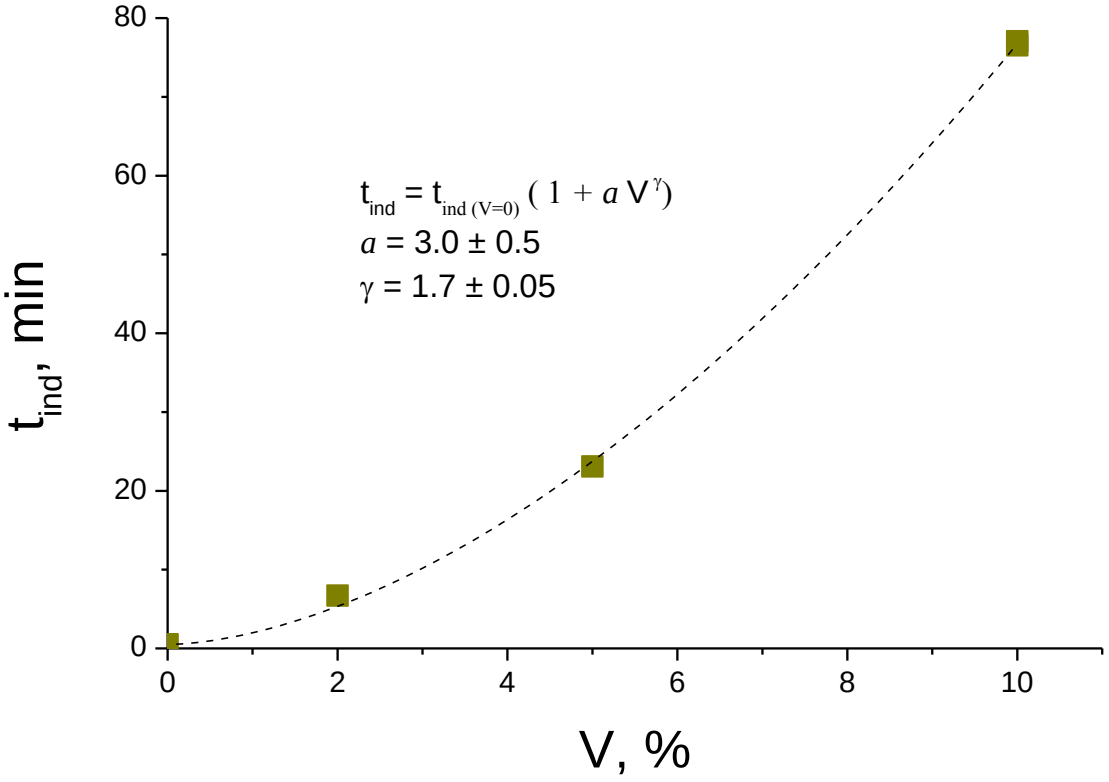

Figure 5: Dependence of induction time on V content (C_0=0.15 mol/l, H=4.5, n-propanol solvent, Re=6000, 20 °C).

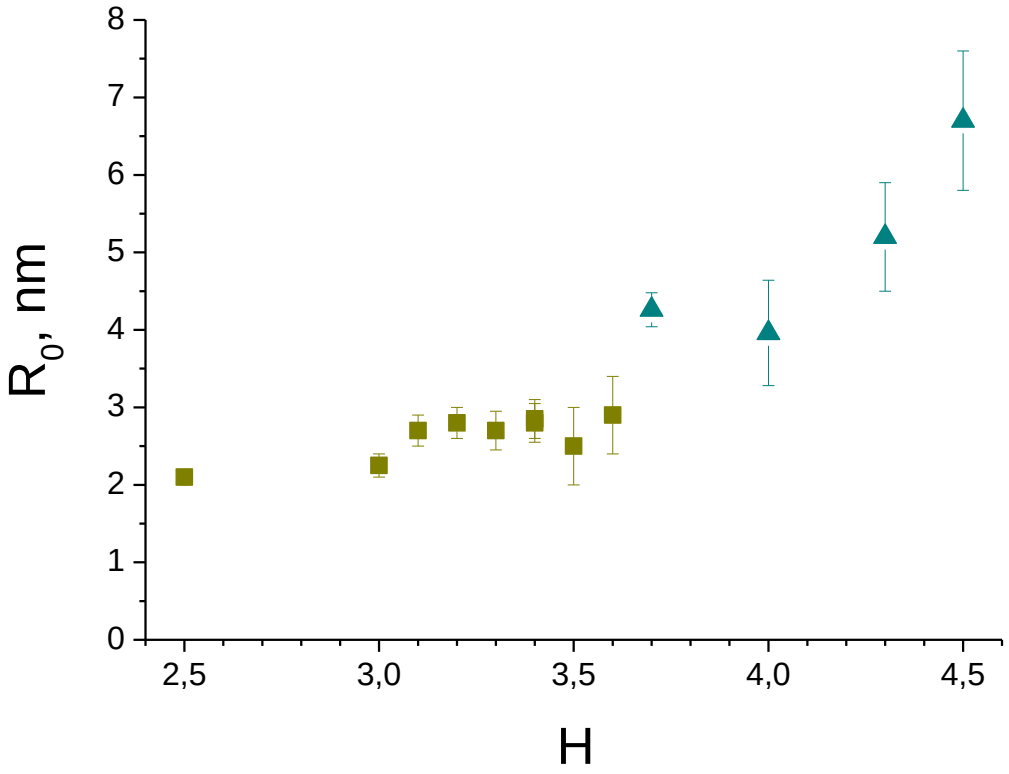

Figure 6: Initial radius of VTOA particles at the induction stage in n-propanol solvent with C_0=0.15 mol/l and vanadium content of 2 mol% (■) and 10 mol% (▲) (Re=6000, 20 °C).

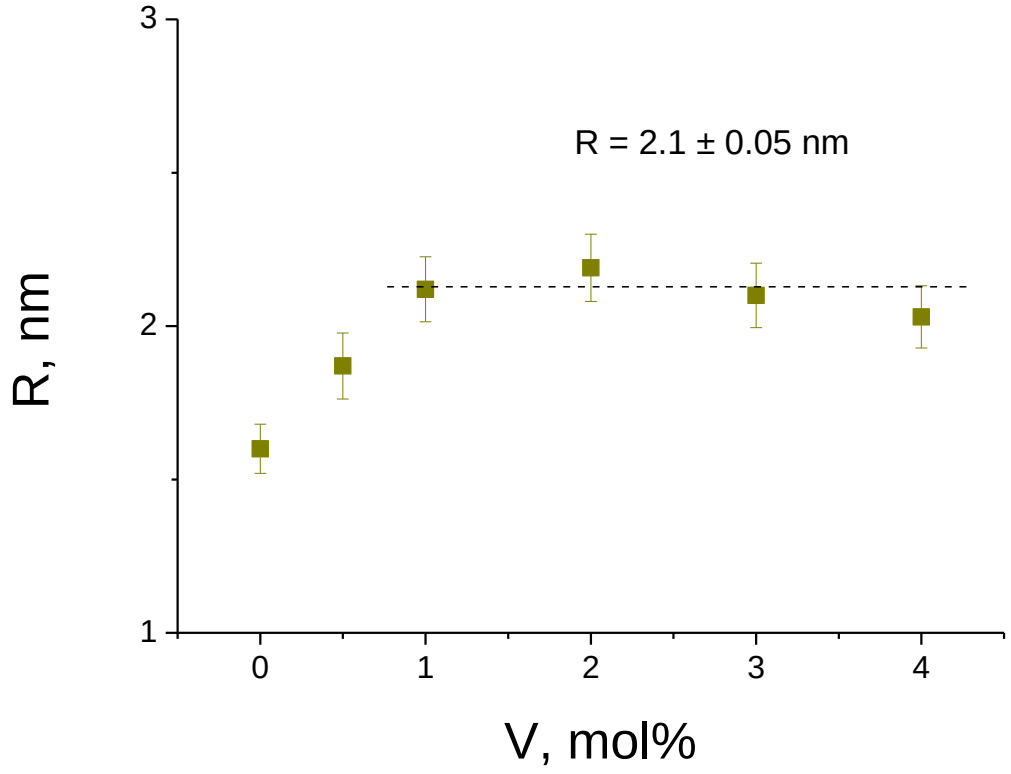

Figure 7: Radius of stable VTOA nanoparticles (nuclei) for different V content (C_0=0.3 mol/l, H=1.6, n-propanol solvent, T=20 °C, Re=6000).

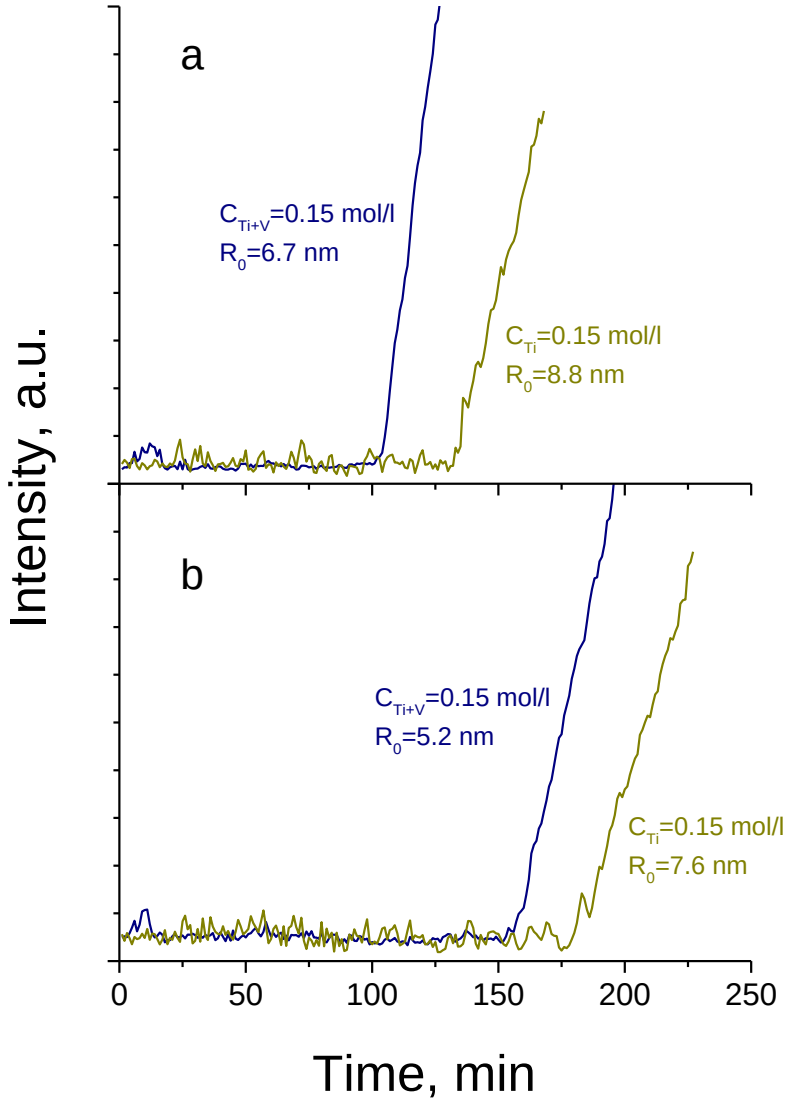

Figure 8: Scattered light intensity during induction period of VTOA nanoparticles growth (Ti:V=9:1, 20 °C) in n-propanol solvent at H=4.5 (a) and H=4.3 (b).

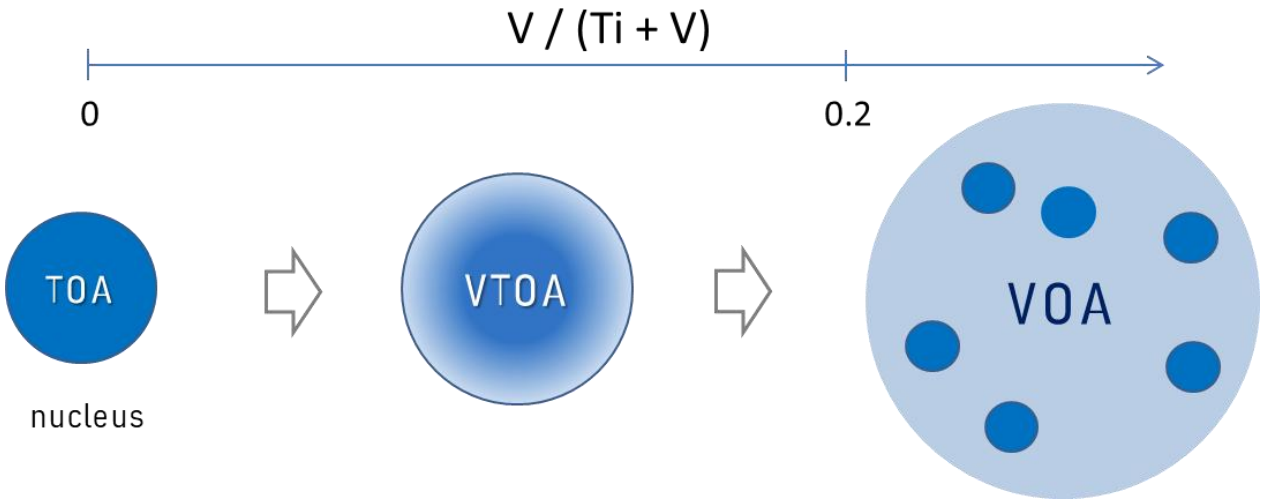

Figure 9: Schema of VTOA species formation.